

# Laboratory determination of the full permeability tensor

Philippe Renard

Institute of Geology, Swiss Federal Institute of Technology, Zürich, Switzerland

Alain Genty<sup>1</sup>

Département de Protection de l'Environnement, Institut de Protection et de Sûreté Nucléaire, Fontenay-aux-Roses, France

Fritz Stauffer

Institute of Hydromechanics and Water Resources Management, Swiss Federal Institute of Technology, Zürich, Switzerland

**Abstract.** Hydraulic conductivity (or intrinsic permeability) determined in a standard permeameter is biased if the anisotropy is not taken into account. This bias can be a significant source of error in the characterization of any type of aquifer or reservoir. Theoretical arguments show that it is possible to determine the complete permeability tensor of a sample by measuring the average filtration velocity and the average gradient vectors during steady state flow experiments. The full permeability tensor is calculated with a linear least squares algorithm. To date, a prototype has been built that shows promising results, but the level of accuracy of the measurements is not yet sufficient to fully demonstrate its applicability. The primary advantages of this new technique are that no preliminary assumptions with respect to the principal directions of anisotropy are required prior to testing and that it does not require sophisticated test equipment.

## 1. Introduction

While clear evidence of the small-scale anisotropy of hydraulic conductivity has been established since the 1950s [*de Boodt and Kirkham*, 1953; *Hutta and Griffiths*, 1955a, 1955b; *Greenkorn et al.*, 1964], most permeameter measurements assume one-dimensional flow inside the sample even when estimating anisotropy [*Auzerais et al.*, 1990; *Hurst and Rosvoll*, 1991; *Burger and Belitz*, 1997]. The main directions of stratifications are identified by visual inspection, and samples are taken parallel and perpendicular to the bedding planes. The directional hydraulic conductivity (scalar) of each sample is determined with a standard permeameter by applying Darcy's law and assuming one-dimensional flow  $K = (Ql)/(A \Delta h)$ , where  $K$  [ $L T^{-1}$ ] is the hydraulic conductivity,  $Q$  [ $L^3 T^{-1}$ ] is the flow rate across the

sample,  $A$  [ $L^2$ ] is the surface perpendicular to flow,  $l$  [ $L$ ] is the length of the sample, and  $\Delta h$  [ $L$ ] is the hydraulic head difference between inlet and outlet. This calculation is correct only if the sample is isotropic, or if the principal axes of anisotropy coincide with the direction of the applied gradient. When these conditions are not met, the hydraulic conductivity can be significantly underestimated. To avoid the assumption of one-dimensional flow and to measure the small-scale anisotropy, different techniques have been proposed and are reviewed by *Rice et al.* [1970], *Bear* [1972, pp. 150–151] or *Bernabé* [1992]. The most convincing experimental technique was published recently by *Bieber et al.* [1996]: they used a point tracer injection and X-ray tomography to observe the shape of the plume inside the sample. If it is a sphere, the medium is isotropic; if it is an ellipsoid the medium is anisotropic. By solving an inverse problem the full tensor of hydraulic conductivity is obtained. However, this technique requires sophisticated equipment thus imparting practical limitations.

The aim of this paper is to propose the theoretical foundations for a new technique. The theory is illustrated through use of a numerical experiment. Some preliminary laboratory results demonstrate the potential of the theory as well as the limitations of our instrumentation.

<sup>1</sup>Now at Département d'Évaluation de Sûreté, Institut de Protection et de Sûreté Nucléaire, Fontenay-aux-Roses, France.

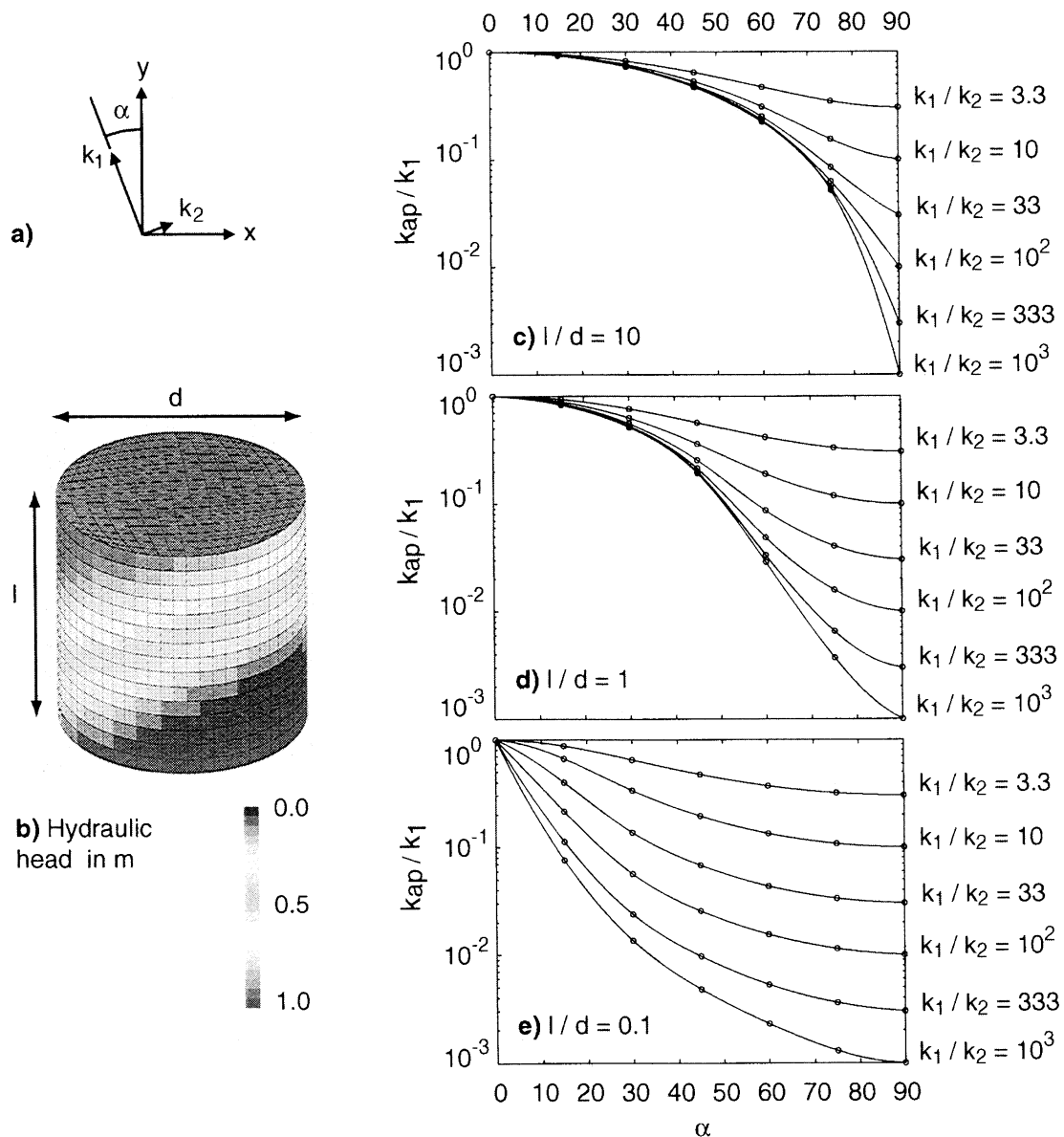


**Figure 1.** Numerical evaluation of the error made by measuring the permeability of an anisotropic sample with a standard permeameter. (a) System of coordinates and principal components of the permeability. (b) Shape of the cylindrical sample showing the finite element discretization as well as the distribution of hydraulic head. (c-e) Ratio of the apparent permeability by the major component of the real tensor ( $k_{ap}/k_1$ ) as a function of the angle  $\alpha$ . The three plots correspond to different shape factors  $l/d$  of the sample.

## 2. Preamble

Before presenting the new methodology, it is worth clarifying what happens when a standard permeameter is used to determine the permeability of an anisotropic medium. For this purpose, we made a series of numerical simulations assuming a cylindrical sample (as is often the case in practice). To simplify the problem, the hydraulic conductivity tensor is assumed to have one major principal component  $k_1$  [ $L T^{-1}$ ] and two identical intermediate and minor principal components  $k_2$  [ $L T^{-1}$ ]. In such a case, the symmetry of the system allows the principal direction of anisotropy to be defined with only one angle  $\alpha$  between the axis

of the cylinder and the direction of  $k_1$  (Figure 1a). The shape of the cylinder is defined by two parameters: its diameter  $d$  [ $L$ ] and its height  $l$  [ $L$ ]. For several combinations of these parameters a numerical simulation with the mixed hybrid finite element code CASTEM [*Commissariat à l'Énergie Atomique, 1997*] was performed to calculate the total flux through the cylinder  $Q$  with a fixed constant head on both ends of the cylinder and to estimate the apparent conductivity  $k_{ap} = (Ql)/[\pi(d/2)^2\Delta h]$ . This value is the conductivity that one would measure with a standard permeameter.

Figure 1b shows the distribution of the hydraulic head for one of the simulations with  $l/d = 1$ . As imposed by the boundary conditions, the top and bottom

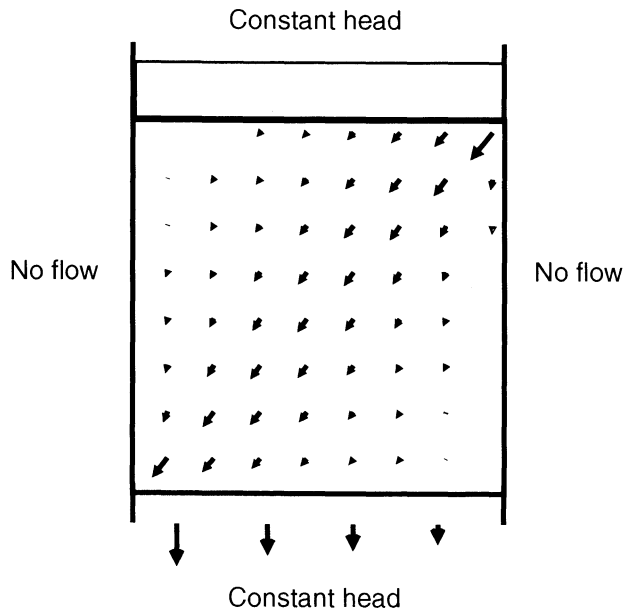


**Figure 2.** Example of the distribution of the specific discharge vectors inside a sample with a principal direction of anisotropy oriented at an angle of  $45^\circ$  with the side of the permeameter and  $l = d$ .

of the cylinder have a constant head, while the distribution along the side of the cylinder (where a no-flow condition is imposed) is tilted. If the sample were isotropic, the head would vary linearly from top to bottom.

Figures 1c, 1d, and 1e show the relative error  $k_{ap}/k_1$  as a function of the dimensionless parameters  $l/d$ ,  $k_1/k_2$ , and  $\alpha$ . When the angle  $\alpha = 0$ ,  $k_1$  is aligned with the axis of the permeameter and the apparent conductivity is equal to the real conductivity. As  $\alpha$  increases, the error becomes a function of  $\alpha$ , of the shape of the sample  $l/d$ , and of the conductivity contrast  $k_1/k_2$ . This error is generally small for small values of  $\alpha$  with elongated samples (Figure 1c) but can significantly increase when the sample has a diameter larger than its height (Figure 1e).

Before presenting the new methodology, it is also important to note that in a standard permeameter the specific discharge vectors are not constant inside the anisotropic sample (as they would be in an isotropic sample) and that they are systematically oriented in a direction imposed by the principal directions of anisotropy (Figure 2). Similarly, the head gradient inside an anisotropic sample varies in space.

### 3. Methodology

In this approach, we define the hydraulic conductivity of the sample as its equivalent hydraulic conductivity tensor  $\mathbf{K}$  (boldface is used to denote vectors and tensors, and italics are used to denote scalars). According to Rubin and Gómez-Hernández [1990],  $\mathbf{K}$  is the constant of proportionality between the averaged head gradient and the averaged specific discharge  $\mathbf{q}$  inside the volume  $V$  of the sample:

$$\frac{1}{V} \int_V \mathbf{q}(\mathbf{x}) dV = -\mathbf{K} \frac{1}{V} \int_V \nabla h(\mathbf{x}) dV, \quad (1)$$

where  $\mathbf{K}$  is a second-order positive tensor and  $\mathbf{x}$  is the space Cartesian coordinate.

This definition requires knowledge of the entire distribution of  $h$  and  $\mathbf{q}$  inside the sample; however, the volume integrals involved in this definition can be replaced by surface integrals [Sánchez-Vila et al., 1995]. For example, the averaged head gradient in the  $x$  direction  $\overline{\nabla h_x}$  (note that the overbar signifies spatial averages) is the scalar product of the averaged gradient by the unit normal vector  $\mathbf{n}_x$  in the  $x$  direction:

$$\overline{\nabla h_x} = \frac{1}{V} \int_V \nabla h \cdot \mathbf{n}_x dV. \quad (2)$$

Integrating by parts allows replacement of the volume integral by a surface integral:

$$\begin{aligned} \overline{\nabla h_x} &= \frac{1}{V} \left[ \int_S h \mathbf{n}_x \cdot \mathbf{n} dS - \int_V h \nabla \cdot \mathbf{n}_x dV \right] \\ &= \frac{1}{V} \int_S h \mathbf{n}_x \cdot \mathbf{n} dS, \end{aligned} \quad (3)$$

where  $S$  is the boundary of the sample,  $\mathbf{n}_x$  is the unit vector in the  $x$  direction, and  $\mathbf{n}$  is the unit vector normal to the elementary surface of integration  $dS$ . Knowing the geometry of the sample and the distribution of heads on its surface is therefore sufficient to calculate the average head gradient inside the sample.

Similarly, the averaged specific discharge in the  $x$  direction  $\overline{\mathbf{q}_x}$  is defined by a volume integral:

$$\overline{\mathbf{q}_x} = \frac{1}{V} \int_V \mathbf{q} \cdot \mathbf{n}_x dV. \quad (4)$$

However, an integration by parts shows that it can be replaced by a surface integral under steady state conditions ( $\nabla \cdot \mathbf{q} = 0$ ):

$$\begin{aligned} \overline{\mathbf{q}_x} &= \frac{1}{V} \left[ \int_S x \mathbf{q} \cdot \mathbf{n} dS - \int_V x \nabla \cdot \mathbf{q} dV \right] \\ &= \frac{1}{V} \int_S x \mathbf{q} \cdot \mathbf{n} dS. \end{aligned} \quad (5)$$

Again, this integral can be easily evaluated knowing the geometry of the sample and measuring the distribution of the fluxes on the boundary of the sample.

At this stage of the methodology, we know that we can determine the components of the averaged specific discharge vector and the components of the averaged head gradient during a flow experiment. The vectorial equation (1) provides a system of three equations with six unknowns: the components of the hydraulic conductivity tensor. This linear system is underdetermined. Because the hydraulic conductivity tensor should be independent of the flow conditions, we propose to use different boundary conditions leading to different flow directions and to calculate the hydraulic conductivity

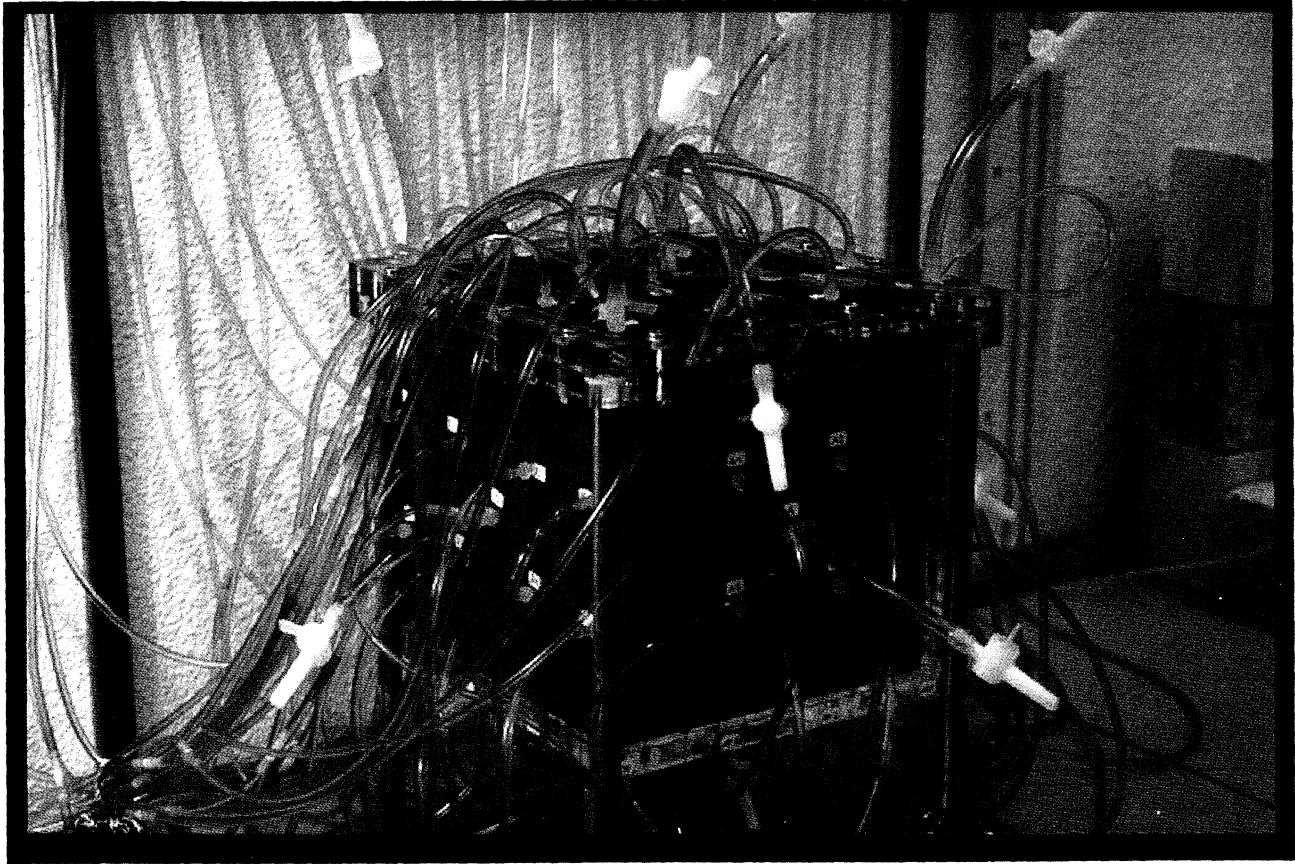


**Plate 1.** Photograph of the full tensor permeameter prototype. In this case, the permeameter is filled with 1cm thick layers of two different types of glass beads inducing an artificial horizontal anisotropy.

tensor which verifies at best, according to least squares criteria, equation (1) for all flow directions. The implementation of the least squares system is discussed in appendix A.

#### 4. A Prototype of a Tensorial Permeameter

To test this methodology, a prototype tensorial permeameter was designed. The system consists of a plexiglass cubic box (inner dimension of 20 cm  $\times$  20 cm  $\times$  20 cm) with a removable top. The lateral walls have a thickness of 1 cm, and the top and bottom walls have a thickness of 1.5 cm. Sixty-two piezometers are evenly distributed on all the faces and the edges of the cube (Plate 1). One circular opening (6.5 mm in diameter) located in the middle of each of the six faces can be used to connect a constant head device. The cube is filled with glass beads. A rubber membrane (2 mm thick) fixed on the cap of the permeameter is used to compress the packing when the permeameter is closed. The experimental procedure involves performing a series of steady state flow experiments by successively applying fixed heads at selected inlet and outlet ports. The head at the inlet is kept constant with a Mariotte bottle. The outlet is kept at atmospheric pressure. The heads are

read on piezometric scales (mm accuracy). Technical difficulties were encountered in obtaining heads at the inlet and outlet ports. As such, a syringe was used, located near the middle of the port just behind the porous medium. The total flux through the sample was measured by weighing the mass of water flowing through the sample for a given period of time.

To calculate the average head gradient and the average specific discharge vector, we have to discretize (3) and (5) taking into account the geometry of the permeameter and the boundary conditions that were imposed. Figure 3a shows a sketch of the permeameter; each face has been labeled from  $S_A$  to  $S_F$ . We consider now the situation where we impose a flow between the centers of face  $S_A$  and  $S_C$ .  $S_1$  denotes the surface of the opening in the center of  $S_A$  where we apply a constant head  $h_1$ , and  $S_2$  denotes the surface of the opening in the center of  $S_C$  where we impose  $h_2$ . Finally,  $S_3$  represents all other boundaries where a no-flow condition exists. In summary, we have the following set of boundary conditions:

$$\begin{aligned}
 \text{Over } S_1 & \quad h = h_1, \\
 \text{Over } S_2 & \quad h = h_2, \\
 \text{Over } S_3 & \quad \mathbf{q} \cdot \mathbf{n} = 0,
 \end{aligned} \tag{6}$$

where  $\mathbf{n}$  is the unit normal vector. Note that  $S = S_1 \cup S_2 \cup S_3$  and  $S = S_A \cup \dots \cup S_F$  are two separate subset patterns of the total surface  $S$  of the cube.  $S_1$  to  $S_3$  represents one pattern corresponding to the hydraulic boundary conditions, while  $S_A$  to  $S_F$  represents a second pattern corresponding to the geometric faces of the cube.

Now, we can calculate the average head gradient. Let us start with the  $x$  component  $\overline{\nabla h_x}$ :

$$\overline{\nabla h_x} = \frac{1}{V} \int_S h \mathbf{n}_x \cdot \mathbf{n} dS. \quad (7)$$

To simplify the surface integral, we need to break it down for each face  $S_A$  to  $S_F$  of the cube. The scalar products of the unit normal vectors  $\mathbf{n}_x$  and the normal vector to the face  $\mathbf{n}$  are equal to zero for the faces  $S_A$ ,  $S_F$ ,  $S_C$ , and  $S_E$ ; and equal to -1 for  $S_D$  and 1 for  $S_B$ . Therefore the averaged head gradient in the  $x$  direction is equal to the difference between the averaged heads on the faces  $S_B$  and  $S_D$  divided by the volume of the cube:

$$\overline{\nabla h_x} = \frac{1}{V} \left( \int_{S_B} h dS - \int_{S_D} h dS \right) \quad (8)$$

or

$$\overline{\nabla h_x} = \frac{\bar{h}_B - \bar{h}_D}{L}, \quad (9)$$

where  $L$  is the length of the edge of the cube and  $\bar{h}_i$  represents the average head on face  $S_i$ ,  $i \in \{A, C, D, E, F\}$ , where

$$\bar{h}_i = \frac{1}{S_i} \int_{S_i} h dS. \quad (10)$$

The components in the  $y$  and  $z$  direction are obtained with:

$$\overline{\nabla h_y} = \frac{\bar{h}_C - \bar{h}_A}{L} \quad (11)$$

$$\overline{\nabla h_z} = \frac{\bar{h}_E - \bar{h}_F}{L}. \quad (12)$$

The components of the average specific discharge vector are obtained in practice by simplifying (5). First, the integral is decomposed in a sum of integrals over the elementary surfaces  $S_1$ ,  $S_2$ , and  $S_3$ . The integral over  $S_3$  vanishes because of the no-flow boundary con-

dition. Then we assume that the coordinates  $(x, y, z)$  are constant over the small inlet and outlet surfaces  $S_1$  and  $S_2$ . We get

$$\begin{aligned} \bar{q}_x &= \frac{Q}{V} (x_1 - x_2), \\ \bar{q}_y &= \frac{Q}{V} (y_1 - y_2), \\ \bar{q}_z &= \frac{Q}{V} (z_1 - z_2), \end{aligned} \quad (13)$$

where  $Q$  is the total flux through the permeameter.

## 5. Numerical Test

Numerical tests were performed in two and three dimensions with different types of boundary conditions, all showing that the methodology works. For illustration purposes, we present only one three-dimensional (3-D) experiment with the same geometry and boundary conditions as the prototype. We meshed the 20-cm side cube with 15,625 regular finite elements. The medium is homogeneous and anisotropic.

We arbitrarily fix the hydraulic conductivity tensor such that it has three different principal components  $k_1 = 100$ ,  $k_2 = 10$ , and  $k_3 = 1$ . We do not give any unit to these conductivities since we are only interested in the comparison between the calculated and reference conductivity. The main axes of anisotropy are obtained through a series of three successive rotations: the first centered around the  $z$  axis with an angle of  $\pi/6$ , the second centered around the  $y$  axis with an angle of  $\pi/3$ , and the third centered around the  $x$  axis with an angle of  $\pi/4$ . Finally, the resulting hydraulic conductivity tensor  $\mathbf{K}_{\text{true}}$  is imposed in the numerical model:

$$\mathbf{K}_{\text{true}} = \begin{pmatrix} 20.125 & -37.2016 & -9.6449 \\ -37.2016 & 79.1875 & 12.9375 \\ -9.6449 & 12.9375 & 11.6875 \end{pmatrix}. \quad (14)$$

Note that the eigenvectors are

$$\begin{aligned} \mathbf{v}_1 &= \begin{pmatrix} -0.433013 \\ 0.883883 \\ 0.176777 \end{pmatrix}, \\ \mathbf{v}_2 &= \begin{pmatrix} -0.250003 \\ -0.3016188 \\ 0.918557 \end{pmatrix}, \\ \mathbf{v}_3 &= \begin{pmatrix} 0.866025 \\ 0.353552 \\ 0.333557 \end{pmatrix}. \end{aligned} \quad (15)$$

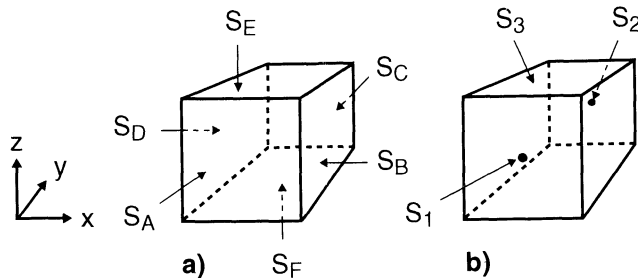


**Figure 3.** Schematic of the new permeameter indicating the two conventions used to name the faces of the cube (a) geometry and (b) boundary conditions.

The flow equation is solved with CASTEM. Plate 2 shows the calculated distribution of heads on the surface of the cube when the center of the faces E and F are the inlet and outlet. On the basis of the calculated

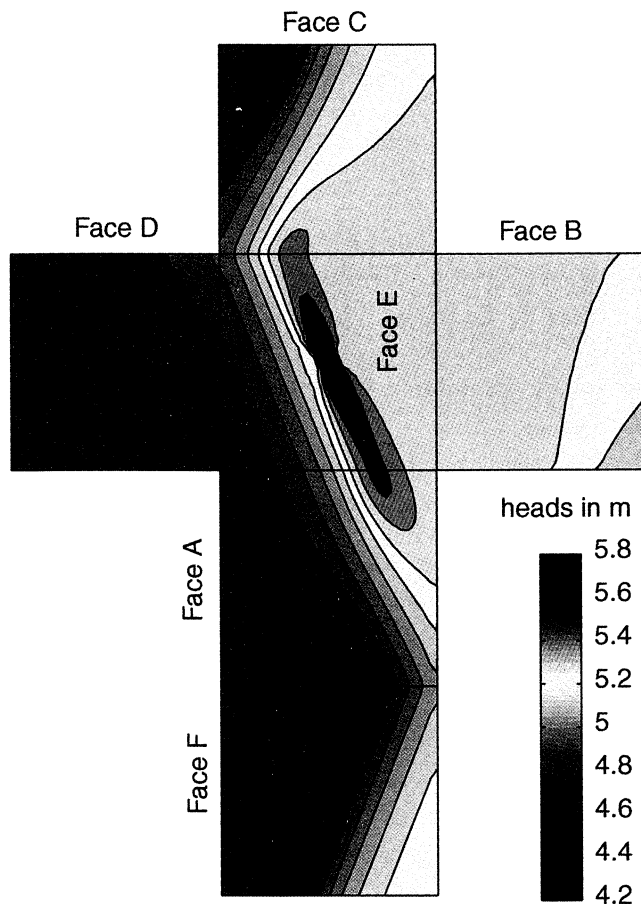


**Plate 2.** Calculated heads distribution displayed on the faces of the permeameter in the case of a full 3-D anisotropy.

heads and fluxes and the application of the proposed methodology we get the following tensor:

$$\mathbf{K}_{\text{est}} = \begin{pmatrix} 20.1364 & -37.2252 & -9.64899 \\ -37.2252 & 79.2364 & 12.946 \\ -9.64899 & 12.946 & 11.6888 \end{pmatrix} \quad (16)$$

with eigenvalues  $k_1 = 100.062$ ,  $k_2 = 9.99985$ , and  $k_3 = 1.00005$ . The eigenvectors are

$$\begin{aligned} \mathbf{v}_1 &= \begin{pmatrix} -0.43301 \\ 0.883888 \\ 0.176761 \end{pmatrix}, \\ \mathbf{v}_2 &= \begin{pmatrix} -0.250008 \\ -0.3016172 \\ 0.918561 \end{pmatrix}, \\ \mathbf{v}_3 &= \begin{pmatrix} 0.866024 \\ 0.353555 \\ 0.333555 \end{pmatrix}. \end{aligned} \quad (17)$$

This numerical example shows that the methodology allows us to estimate correctly the tensor of hydraulic conductivity. The calculated tensor is very close to the original, and the eigenvalues and eigenvectors are also very well reproduced.

All our numerical experiments with isotropic and anisotropic homogeneous media, in two and three dimensions, systematically show an excellent agreement between the input hydraulic conductivity tensor and the estimated one. Tests with heterogeneous stratified media also provide good results [Renard, 1998].

## 6. Laboratory Experiments

Using the prototype, we conducted three series of experiments. In the first experiment the permeameter was filled with an homogeneous packing of 1-mm-diameter glass beads. In the second experiment we made 1-cm-thick horizontal strata by alternating 1-mm-diameter glass beads and smaller beads having diameters between 0.4 and 0.6 mm. In the third experiment the permeameter was filled with 1-mm glass beads partitioned by with five plastic sheets having specific holes and oriented at an angle of  $18.8^\circ$  with the horizontal plane (Figure 4). For each case, at least three flow experiments along the three principal directions were conducted.

For each experiment, special care was taken in packing the beads. We used a sand raining procedure already reported by Stauffer and Dracos [1986]. A special apparatus was employed. The beads were funneled into this device where they fall freely for a fixed distance

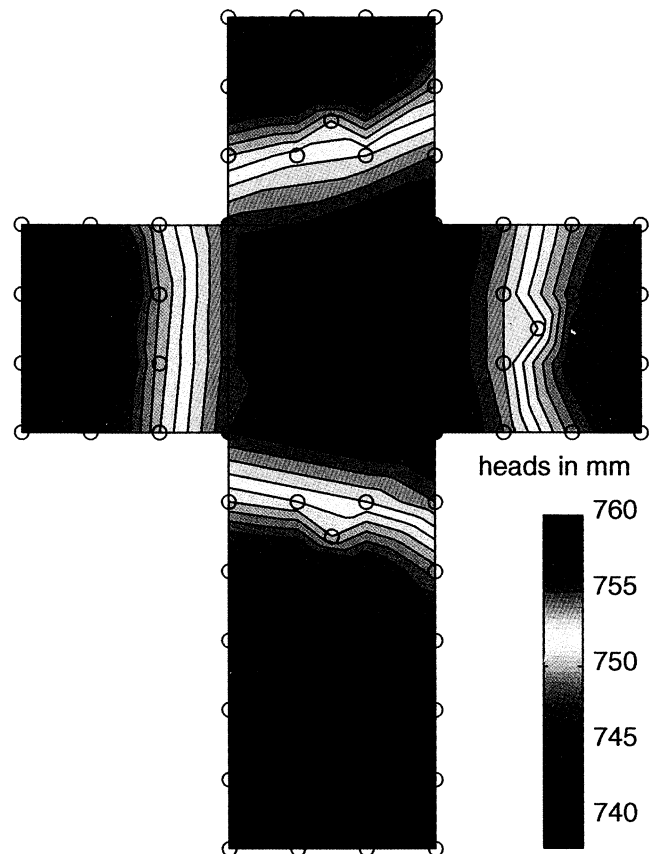


**Plate 3.** Distribution of measured hydraulic heads. The circles correspond to the locations of the measurements. The isolines are obtained by linear interpolation between the measurements.

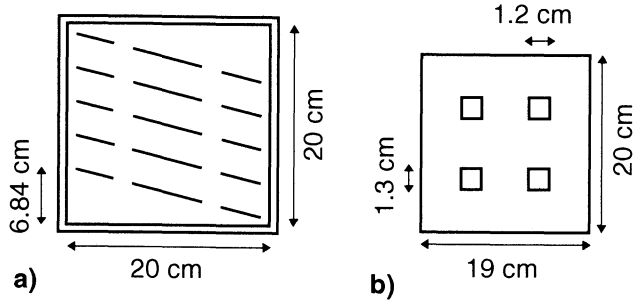


**Figure 4.** Schematic of the technique used to create an artificial inclined anisotropy with five plastic sheets. (a) Vertical cross section through the permeameter (parallel to face A). (b) Map view of the plastic sheets with the four openings.

and then pass through a series of sieves before reaching the surface of the packing. With this method, a dense packing is produced. For the tensorial permeameter we had to position and move this device manually because its diameter was smaller than the surface of the permeameter. The medium is then flushed with  $\text{CO}_2$  to avoid trapping air bubbles. Finally, the medium is slowly saturated with water from bottom to top.

To check the results of the tensorial permeameter, we need to have reference values. For this purpose, the hydraulic conductivity of each glass bead packings was measured independently with a standard cylindrical permeameter. The packings were made with the same tool and procedure as that for the tensorial permeameter. For each packing, a series of six to nine experiments with different head gradients were realized. For each experiment the propagation of head gradients and flow rates uncertainties are calculated. The hydraulic conductivity and its uncertainty are obtained with a standard least squares procedure. The conductivities that we obtain are  $(9.5 \pm 0.7) \times 10^{-3}$  m/s for the 1-mm beads and  $(2.08 \pm 0.05) \times 10^{-3}$  m/s for the 0.4- to 0.6-mm beads. In the same device we determined the conductivity perpendicular to the layers of the horizontally stratified media:  $(3.1 \pm 0.2) \times 10^{-3}$  m/s. This is in agreement with the harmonic average of the conductivities of the two types of medium with a smaller error bar than the calculated value:  $(3.4 \pm 0.5) \times 10^{-3}$  m/s. The reference conductivity parallel to the layers was calculated by taking the arithmetic mean of the two conduc-

tivities and propagating the errors:  $(5.8 \pm 0.4) \times 10^{-3}$  m/s.

Now we report the results of the third series of experiments in the tensorial permeameter involving the inclined anisotropy. Plate 3 shows the distribution of the hydraulic heads on the surface of the sample. The influence of anisotropy is clearly visible since the isolines of constant head are not parallel to the edges of the cube but inclined. Applying the proposed methodology to the measurements, we get

$$\mathbf{K}_{est} = \begin{pmatrix} 30 \pm 5 & -0.6 \pm 0.6 & -0.7 \pm 0.7 \\ -0.6 \pm 0.6 & 21 \pm 7 & 2 \pm 1 \\ -0.7 \pm 0.7 & 2 \pm 1 & 14 \pm 2 \end{pmatrix} \times 10^{-3} \text{ (m/s)}. \quad (18)$$

The uncertainties are calculated through the propagation of errors due to head measurements and interpolation. The eigenvectors of the tensor are oriented such that the principal direction of anisotropy is inclined with an angle of  $16^\circ$  with the horizontal direction. This is encouraging since we expect an angle of  $19^\circ$ . Furthermore, from the calculation we obtain a nonzero  $K^{yz}$  value.  $K^{xy}$  and  $K^{xz}$  are not significantly different from zero, which is expected. However, the eigenvalues are not satisfactory ( $k_1 = 3.0 \times 10^{-2}$  m/s,  $k_2 = 2.1 \times 10^{-2}$  m/s and  $k_3 = 1.3 \times 10^{-2}$  m/s). The reference for the 1-mm glass beads is  $(9.5 \pm 0.7) \times 10^{-3}$  m/s. The first two components are too large and are not equal, as they should be. The third component is smaller than the first two but again is too large compared to the reference conductivity.

The results of the experiments conducted with the isotropic and horizontally stratified media are presented in Table 1. The off-diagonal values of the tensors approximate zero. The principal direction of anisotropy are parallel to the coordinate axes and therefore are correctly identified. However, the eigenvalues are not correctly determined. There is a general tendency to overestimate them.

## 7. Discussion

Both theoretical and numerical arguments show that it is possible to determine the full permeability tensor of

**Table 1.** Comparison of Components of Hydraulic Conductivity Tensor Determined with Tensorial Permeameter and Reference Values<sup>a</sup>

	$K^{xx}$	$K^{yy}$	$K^{zz}$	$K^{xy}$	$K^{xz}$	$K^{yz}$
Isotropic	$29 \pm 5$	$12 \pm 3$	$15 \pm 3$	$-0.3 \pm 0.5$	$0.3 \pm 0.5$	$0.2 \pm 0.3$
Reference	$9.5 \pm 0.7$	$9.5 \pm 0.7$	$9.5 \pm 0.7$	0	0	0
Stratified	$12 \pm 2$	$10 \pm 3$	$7.5 \pm 1.3$	$0.1 \pm 0.1$	$0.03 \pm 0.1$	$-0.07 \pm 0.09$
Reference	$5.8 \pm 0.4$	$5.8 \pm 0.4$	$3.1 \pm 0.2$	0	0	0

<sup>a</sup>In mm/s. Errors correspond to the 68% confidence limit interval.

a sample with a series of at least three steady state flow experiments. The methodology is simple. Compared to existing technology, this approach presents several advantages: (1) it does not assume a priori any principal direction of anisotropy; (2) it does not mix the effect of anisotropy and heterogeneity since the tensor is measured directly for a given sample and not constructed after measuring the conductivity of orthogonal samples; (3) it does not require modification of the geometry of the sample between different flow experiments as is required in the techniques proposed by *Moore* [1979] or *Rose* [1982]; (4) it does not require the numerical solution of a complete inverse problem as proposed by *Bernabé* [1992] or *Bieber et al.* [1996]; (5) it does not require a highly sophisticated apparatus such as that used in the tracer injection method [*Bieber et al.*, 1996]; and (6) the theory is not limited to a particular sample shape or special boundary conditions, but is limited by its ability to measure or to impose a distribution of heads and fluxes along the boundary of the sample.

Despite these advantages and the excellent results obtained with the numerical examples, the results of the laboratory experiments are somewhat disappointing. The eigenvalues of the permeability tensor were always estimated with a rather large error compared to the expected results; that is, the references often do not fall within the error bars of the measurements. We also obtain significant anisotropy between  $K^{xx}$ ,  $K^{yy}$ , and  $K^{zz}$  when we do not expect it. We can ask: Are the estimated uncertainties too small or the references incorrect?

Let us discuss first the estimation of the uncertainties. The uncertainties are much smaller for the average specific discharge components ( $\sim 2\%$ ) than for the head gradients ( $\sim 25\%$ ).

For the specific discharge the sources of uncertainty are the techniques used to measure the time and the mass of fluid flowing through the permeameter. For the head gradients, there are several sources of uncertainty: imprecise reading of piezometer heads (2 mm uncertainty), errors of head measurements in the inlet and outlet ports due to local effects, and errors when linearly interpolating the heads from the 17 measurements. The interpolation error is a function of the shape of the head distribution at the face. It is estimated with the numerical model to be  $\sim 10\%$  to  $20\%$  for the head gradient in the direction of flow and to be  $< 2\%$  for the head gradient in the perpendicular direction. For the inlet and outlet ports we observe that the heads measured are strongly affected by unpredictable local phenomena. Sixty percent of our experiments for the isotropic case show an important asymmetry in the head drop at the inlet and the outlet port. For example, we can generate a head of 140 cm at the inlet, an average head of 60 cm in the media, and a head of 40 cm at the outlet. This asymmetry is not systematic and is not related to specific inlet or outlet ports. We interpret the asymmetry as a result of localized effects around the ports creating

an artificial conductance or resistance where the flow is concentrated. We estimated this error by analyzing the asymmetry of all experiments on isotropic media and obtained 20 cm. Finally, the error on the head gradient in the main flow direction is dominated by the interpolation error and by the local effects at the inlet and outlet ports. We estimate the total uncertainty to be around 25%. The errors on the head gradient in the directions perpendicular to the flow are much smaller. They are dominated by reading errors. We estimate the absolute error in this case to be around 2 mm.

Could the reference be incorrect? Several phenomena can affect the reference. First, we may have created an artificial anisotropy by manually moving the sand raining device above the permeameter while filling it. Second, the packing may be less dense in the tensorial permeameter than in the standard permeameter because we had to move the sand raining device. We cannot quantify the potential errors of these two phenomena, but if they affect our experiments, they would likely produce higher conductivities in the tensorial permeameter than in the standard one. Third, the plexiglass walls of the tensorial permeameter may be deforming during the flow experiment, creating additional void space and artificially increasing the apparent conductivity. We calculated that the maximum deflection at the center of the walls to be  $\sim 0.2$  mm for the lateral walls and 0.04 mm for the top and bottom walls. To estimate the possible influence of this deformation on the apparent conductivity of the medium, we assume the following: we neglect the deformation of the top and bottom; we sum up all the additional void space, and we calculate an average aperture corresponding to a single plane fracture representing the total void space; we then calculate the flow through this fracture with Poiseuille's law. In doing so, we obtain a mean aperture of 0.53 mm and an increase in the apparent conductivity of the medium equal to  $6.2 \times 10^{-4}$  m/s. The apparent conductivity could then increase from  $9.5 \times 10^{-3}$  to  $11 \times 10^{-3}$  m/s. This still does not help explain the value of  $29 \times 10^{-3}$  m/s that we obtained for  $K^{xx}$  for the isotropic case. Furthermore, our estimation of the increase in conductivity is probably an overestimation since the packing is compressed by the rubber membrane along the top and because the total deformation is not concentrated along a single plane.

Therefore, if we believe that the reference is acceptable, then we must conclude that the errors are not estimated properly. Then we can question the validity of our experimental observations: Did we really observe a significantly nonzero crossterm?

As a final remark, it is important to realize that the uncertainty of the head gradient has a high impact on the tensor of conductivity. We investigated this problem numerically and in particular the problem of insufficient data to calculate the average head on the faces of the sample. For example, if we take the theoretical numerical example of section 5 for which we know the reference

conductivity as well as the calculated head distribution on the faces of the cube, if we sample the heads at the position of the actual piezometers to estimate the mean heads, and if we apply our technique to get the conductivity tensor, we then obtain the eigenvalues:  $k_1 = 25$ ,  $k_2 = 7.4$ , and  $k_3 = 0.96$  instead of 100, 10, and 1.

## 8. Conclusion

This paper presents an innovative and simple technique for determining the full hydraulic conductivity tensor of a sample in the laboratory. The main motivation is not necessarily to obtain the tensor itself (which may or may not be representative of a large domain) but to avoid significant measurement errors that can occur in a standard permeameter when the anisotropy is not aligned with the axes of the sample.

The theory is general, and it does not require special boundary conditions or a particular shape for the sample. The numerical experiments show that the theory gives excellent results. Unfortunately, our laboratory experiments are not conclusive. We may have been able to detect a significant cross term of the conductivity tensor for an inclined anisotropy, but this may also be due to measurement errors. It is therefore necessary to pursue the experimental work to reduce the uncertainty and to provide a clear answer to the question: Is it possible to use this technique in practice or is it just a beautiful but useless theoretical idea?

## Appendix A: The Least squares Formulation

In the general case, the system of equations to determine the conductivity tensor is a multiple regression problem. The discharge is a function of three head gradients. The general least squares system is available from Renard [1998].

In the specific case of the prototype that we are discussing here, we can simplify considerably the least squares problem because for each experiment there is only one component of the discharge vector which is not zero. We also know (see section 7) that the uncertainty of head gradients is much larger than the uncertainty of the discharge. Therefore we write the flow equations in term of resistivity instead of conductivity, and we can separate the least squares equations for every component of the resistivity tensor:

$$\overline{\nabla h_u}^i = -R_{uv} \overline{q_v}^i, \quad (\text{A1})$$

where  $i \in 1, \dots, n$  is an index over the experiments and  $u, v \in \{x, y, z\}^2$  are indices over the directions. To respect the symmetry of the tensor, we impose  $R_{uv} = R_{vu}$ . In the end, we have to solve six standard linear least squares systems to get the six components of the tensor and their respective uncertainties. The conductivity tensor is obtained by inverting the resistivity

tensor, and the uncertainties are obtained by propagating analytically the uncertainty through the matrix inversion.

**Acknowledgments.** The authors gratefully acknowledge Michael Knüsel and Benoit Guivarc'h, who managed the construction of the device and conducted the experiments in the laboratory. We sincerely thank Stephen Brown and Vincent Tidwell for their very constructive reviews. Thanks to Ivan Lunati for contributing many valuable comments on error analysis and to Wolfgang Kinzelbach for offering the laboratory space and motivating discussions. Finally, this research was funded partly by the Swiss Federal Institute of Technology and partly by the IPSN through the cooperation contract 4060 200 8B065670/SH.

## References

- Auzerais, F. M., D. V. Ellis, S. M. Luthi, E. B. Dussan, and B. J. Pinoteau, Laboratory characterization of anisotropic rocks, paper SPE 20602 presented at 65th Annual Technology Conference and Exhibition, Soc. of Pet. Eng., New Orleans, La., 1990.
- Bear, J., *Dynamics of Fluids in Porous Media*, 764 pp., Dover, Mineola, N.Y., 1972.
- Bernabé, Y., On the measurement of permeability in anisotropic rocks, in *Fault Mechanics and Transport Properties of Rocks*, edited by B. Evans and T.-F. Wong, 147-167, Academic, San Diego, Calif., 1992.
- Bieber, M. T., P. Rasolofosaon, B. Zinszner, and M. Zamora, Measurement and overall characterization of permeability anisotropy by tracer injection, *Rev. Inst. Fr. Pet.*, 51(3), 333-347, 1996.
- Burger, R. L., and K. Belitz, Measurement of anisotropic hydraulic conductivity in unconsolidated sands: A case study from a shoreface deposit, Oyster, Virginia, *Water Resour. Res.*, 33(6), 1515-1522, 1997.
- Commissariat à l'Energie Atomique (CEA), CASTEM2000 user's manual, English version, technical report, Saclay, France, 1997.
- de Boodt, M. F., and D. Kirkham, Anisotropy and measurements of air permeability of soil clods, *Soil Sci.*, 76, 127-133, 1953.
- Greenkorn, R. A., C. R. Johnson, and L. K. Shallenberger, Directional permeability of heterogeneous anisotropic porous media, *Soc. Pet. Eng. J.*, 4, 124-132, 1964.
- Hurst, A., and K. J. Rosvoll, Permeability variations in sandstones and their relationship to sedimentary structures, in *Reservoir Characterization II, Orlando*, edited by L. W. Lake, H. B. Carroll, and T. C. Wesson, 166-196, Academic, San Diego, Calif., 1991.
- Hutta, J. J., and J. C. Griffiths, Directional permeability of sandstones; a test of technique, *Prod. Mon.*, 19(11), 26-34, 1955a.
- Hutta, J. J., and J. C. Griffiths, Directional permeability of sandstones; a test of technique, *Prod. Mon.*, 19(12), 24-31, 1955b.
- Moore, P. J., Determination of permeability anisotropy in a two-way permeameter, *Geotech. Test. J.*, 2(3), 167-169, 1979.
- Renard, P., A modified permeameter to determine the full hydraulic conductivity tensor, in *Gambling With Groundwater - Physical, Chemical, and Biological Aspects of Aquifer-Stream Relations*, edited by J. V. Brahana et al., 727-733, Am. Inst. of Hydrol., St. Paul, Minn., 1998.
- Rice, P. A., D. J. Fontugne, R. G. Latini, and A. J. Barduhn, Anisotropic permeability in porous media, *Ind. and Eng. Chem.*, 62(6), 23-31, 1970.

- Rose, W. D., A new method to measure directional permeability, *J. Pet. Technol.*, 34, 1142-1144, 1982.
- Rubin, Y., and J. Gómez-Hernández, A stochastic approach to the problem of upscaling of conductivity in disordered media: Theory and unconditional numerical simulations, *Water Resour. Res.*, 22(4), 691-701, 1990.
- Sánchez-Vila, X., J. P. Girardi, and J. Carrera, A synthesis of approaches to upscaling of hydraulic conductivities, *Water Resour. Res.*, 31(4), 867-882, 1995.
- Stauffer, F., and T. Dracos, Experimental and numerical study of water and solute infiltration in layered porous media, *J. of Hydrol.*, 84(1/2), 9-34, 1986.
- General Leclerc, BP 6, 92265 Fontenay-aux-Roses Cedex, France. (e-mail: genty@mercure.far.cea.fr)
- P. Renard, Institute of Geology, Swiss Federal Institute of Technology, CH-8093 Zürich, Switzerland. (e-mail: renard@erdw.ethz.ch)
- F. Stauffer, Institute of Hydromechanics and Water Resources Management, Swiss Federal Institute of Technology, CH-8093 Zürich, Switzerland. (e-mail: stauffer@ihw.baug.ethz.ch)

---

A. Genty, Institut de Protection et de Sûreté Nucléaire, Département d'Évaluation de Sûreté, 60-68 Avenue du

(Received September 11, 2000; revised April 17, 2001; accepted June 30, 2001.)